Inorganic Chemistry

Article

pubs.acs.org/IC

Photorelease and Cellular Delivery of Mitocurcumin from Its Cytotoxic Cobalt(III) Complex in Visible Light

Aditya Garai,[†] Ila Pant,[‡] Samya Banerjee,[†] Bhabatosh Banik,[†] Paturu Kondaiah,*[,‡] and Akhil R. Chakravarty*[,†]

[†]Department of Inorganic and Physical Chemistry, Indian Institute of Science, Bangalore 560012, India

[‡]Department of Molecular Reproduction, Development and Genetics, Indian Institute of Science, Bangalore 560012, India

Supporting Information

ABSTRACT: Ternary cobalt(III) complexes of curcumin (Hcur) and mitocurcumin [Hmitocur, a dicationic bis-(triphenylphosphonium) derivative of curcumin] having a tetradentate phenolate-based ligand (H_2L), namely, [Co(cur)(L)] (**1**) and [Co(mitocur)(L)]Cl_2 (**2**), were prepared and structurally characterized, and their photoinduced cytotoxicity was studied. The diamagnetic cobalt(III) complexes show an irreversible Co(III)−Co(II) redox response and a quasireversible curcuminoid-based reduction near −1.45 and −1.74 V SCE, respectively, in DMF/0.1 M [^{n}Bu$_4$N](ClO$_4$). The complexes exhibit a curcumin/mitocurcumin-based absorption band near 420 nm. Complex **1** was structurally characterized by X-ray crystallography. The structure contains the metal in a CoN_2O_4 distorted octahedral coordination arrangement with curcumin binding to the metal in its enolic form. Binding to cobalt(III) increases the hydrolytic stability of curcumin. Complex **2**, having a dicationic curcuminoid, shows significant cellular uptake and photoinduced cytotoxicity compared to its curcumin analogue **1**. The dicationic cobalt(III) complex **2** has significantly better cellular uptake and bioactivity than the neutral species **1**. Complex **2** with mitochondrial localization releases the mitocurcumin dye upon exposure to visible light (400−700 nm) in human breast cancer MCF-7 cells through photoreduction of cobalt(III) to cobalt(II). Complex **2** displays a remarkable photodynamic therapy (PDT) effect, giving an IC_{50} value of ∼3.9 μM in visible light (400−700 nm) in MCF-7 cells while being much less toxic in the dark (>50 μM). The released mitocurcumin acts as a phototoxin, generating intracellular reactive oxygen species (ROSs). The overall process leads to light-controlled delivery of a curcuminoid (mitocur) into the tumor cells while the dye alone suffers from hydrolytic instability and poor bioavailability.

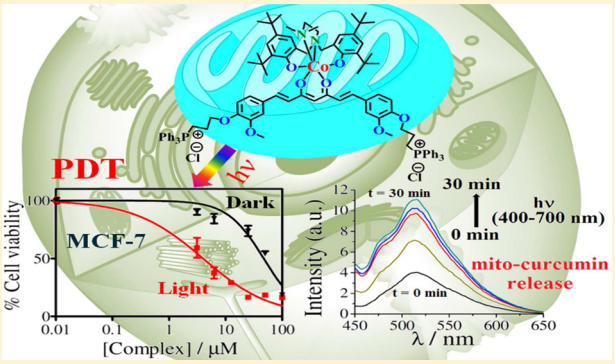

INTRODUCTION

As the naturally occurring polyphenolic active ingredient of turmeric, curcumin is well-known for its anticancer activity and other medicinal values.[1,2] It induces apoptosis in tumor cells by interfering with the activity of the transcription factor NF-κB. It enhances the activity of the major tumor suppressor protein p53.[3,4] However, the clinical use of curcumin (Hcur), 1,7-bis(4-hydroxy-3-methoxyphenyl)-1,6-hepta-diene-3,5-dione, is severely limited because of its poor bioavailability and hydrolytic instability under physiological conditions. This is attributed to the presence of a β-diketone moiety in its structure that is susceptible to hydrolysis, leading to its rapid degradation.[1,5] Although several modifications of the dye have been made to improve its efficacy without much success, one strategy that has been found to be effective is the covalent binding of curcumin in its enolic form as a monoanionic *O,O*-donor chelating ligand to an oxophilic metal ion.[6−18] The coordination chemistry of curcumin complexes is of considerable importance because of their remarkable anticancer activity with vastly improved hydrolytic stability of curcumin.[6−10] Such complexes show excellent photocytotoxicity in visible light in a variety of cancer cells.[10−18] Thus, curcumin as a photosensitizer with a visible band near 440 nm and as a fluorescent tag for its green emission property is suitable for dual cellular applications: (i) imaging cells to study the intracellular localization of the metal complexes and (ii) killing cancer cells upon irradiation with visible light (400−700 nm) by generating reactive oxygen species (ROSs).[10] The chemistry of curcumin in the photodynamic therapy (PDT) of cancer as such or in its metal-bound form is an emerging area because of the novel photophysical properties and photosensitizing ability of curcumin.[10−17] PDT is a noninvasive therapeutic modality to treat cancer by involving the activation of a photosensitizer in visible light to generate reactive oxygen species (ROSs) that selectively kill the light-exposed cancer cells, leaving unexposed healthy cells unaffected.[18−23] PDT reduces the drug-related toxicity on human organs compared to that induced by the conventional platinum-based chemotherapeutic drugs. Different types of

Received: March 4, 2016

DOI: 10.1021/acs.inorgchem.6b00554
Inorg. Chem. XXXX, XXX, XXX−XXX

metal-based PDT agents have been reported in recent years.[24−33]

Sadler and co-workers developed six-coordinate platinum(IV)-based photoactivated chemotherapeutic (PACT) agents that, upon light activation, release two axial ligands to generate planar platinum(II) active species.[34,35] Lippard and co-workers reported six-coordinate nontoxic platinum(IV) complexes that, upon intracellular reduction, release their axial ligands to generate four-coordinate active platinum(II) species.[36,37] This concept of releasing ligands from the coordination sphere of a metal ion from its higher oxidation state to a lower one by chemical or photochemical means could be used for the successful delivery of curcumin inside cells, thus increasing its bioavaiability and hydrolytic stability in a significant way. Hambley and co-workers recently reported the release of curcumin at the target site from its ternary cobalt(III) complexes.[18] As for the platinum(IV) complexes, the release of curcumin is effected by intracellular reduction of cobalt(III) to cobalt(II) with a concomitant structural change.[9] Again, similarly to the platinum(IV) prodrugs, the reduction of the metal with ligand loss can be achieved by photoirradiation.[18,38] Delivery of curcumin at the target site by photochemical means seems to be a convenient option compared to other modes of using nanoparticles, liposomes, and micellar systems.[9,18,38] The present work stems from our interest in probing the cobalt(III) chemistry of curcumin. We have designed and synthesized new ternary cobalt(III) complexes of curcumin (Hcur) and mitocurcumin (Hmitocur) using a dianionic tetradentate ancillary ligand (H_2L) with the objective of releasing curcumin upon photoirradiation using visible light (Figure 1). The choice

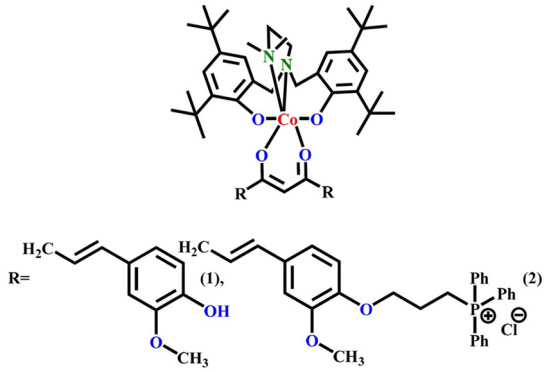

Figure 1. Molecular structures of cobalt(III) complexes **1** and **2** and the ligands used.

of mitocurcumin with two cationic triphenylphosphonium (TPP) moieties appended to the curcumin core was intended to direct the complex to the mitochondria of the cells, instead of the nucleus, for improved activity and to avoid the nuclear excision repair (NER) mechanistic pathway.[39−41] The tetradentate phenolate-based ligand (H_2L) was used to impart stereochemical rigidity and to augment the lipophilicity of the complexes.

Herein, we describe the synthesis, characterization, crystal structure, and photoinduced cytotoxicity of ternary curcumin (Hcur) and dicationic mitocurcumin (Hmitocur) cobalt(III) complexes of a phenolate-based ligand (H_2L), namely, [Co(cur)(L)] (**1**) and $[Co(mitocur)(L)]Cl_2$ (**2**) (Figure 1). The significant results of this work include (i) reporting the first crystal structure of a cobalt complex of curcumin; (ii) observing the enhancement of the hydrolytic stability of curcumin upon binding to the cobalt(III) metal center; (iii) developing a mitocurcumin complex (complex **2**) that shows selective mitochondrial localization and visible-light- (400−700 nm) induced release of the dye inside cancer cells (MCF-7, human breast cancer) with concomitant metal reduction; (iv) obtaining a remarkable PDT effect of complex **2**, comparable to that of photofrin, giving an IC_{50} value of ∼3.9 μM in the light (400−700 nm) in MCF-7 cells while being less toxic in the dark; and (v) achieving higher cellular uptake of the dicationic complex **2** compared to the charge-neutral curcumin complex **1**, thus highlighting the importance of the structure−activity relationship (SAR) in this class of cobalt(III) complexes.

EXPERIMENTAL SECTION

Materials and Measurements. The reagents and chemicals were obtained from various commercial sources (s.d. Fine Chemicals, Mumbai, India; Sigma-Aldrich, St. Louis, MO) and used as received. Solvents were purified according to literature procedures.[42] 2′,7′-Dichlorofluoresceindiacetate (DCFDA), 3-(4,5-dimethylthiazol-2-yl)-2,5-diphenyltetrazolium bromide (MTT), propidium iodide (PI), Dulbecco's modified eagle medium (DMEM), Dulbecco's phosphate-buffered saline (DPBS), and fetal bovine serum (FBS) were purchased from Sigma (St. Louis, MO). MitoTracker Red was purchased from Invitrogen (Carlsbad, CA). The bis(triphenylphosphonium) derivative of (1*E*,6*E*)-1,7-bis(4-hydroxy-3-methoxyphenyl)-1,6-heptadiene-3,5-dione (curcumin) dichloride (the dichloro salt of dicationic mitocurcumin, Hmitocur) and the tetradentate ligand, namely, 6,6′-(((2-(dimethylamino)ethyl)azanediyl)bis(methylene))bis(2,4-di-*tert*-butylphenol) (H_2L), were synthesized by the reported procedures (Schemes S1 and S2 in the Supporting Information).[39]

Elemental analyses were performed on a Thermo Finnigan Flash EA 1112 CHN analyzer. The electronic and infrared spectra were recorded on a Perkin-Elmer Spectrum One 55 spectrophotometer and a Perkin-Elmer Lambda 35 IR spectrometer, respectively. Fluorescence spectra were obtained using a Perkin-Elmer LS 55 spectrophotometer. ^{1}H NMR spectra were recorded at room temperature on a Bruker 400 MHz NMR spectrometer. Molar conductivity measurements were done using a Control Dynamics (Ankleshwar, India) conductivity meter. Cyclic voltammetric measurements were carried out at 25 °C on an EG&G PAR model 253 VersaStat potentiostat/galvanostat using electrochemical analysis software 270 in a three-electrode configuration consisting of a glassy carbon working electrode, a platinum wire auxiliary electrode, and a saturated calomel reference electrode (SCE) in dimethylformamide (DMF) with tetrabutylammonium perchlorate (TBAP, 0.1 M) as a supporting electrolyte. The redox data were uncorrected for junction potentials. Electrospray ionization (ESI) mass spectral measurements were made using an Agilent Technologies 6538 UHD Accurate-mass Q-TOF LC/MS and BrukerDaltonics Esquire 300 Plus ESI model mass spectrometers. Magnetic susceptibility measurements of the samples at 298 K were done using a magnetic susceptibility balance from Sherwood Scientific (Cambridge, U.K.). Flow cytometric analysis was done on a FACSCalibur Becton Dickinson (BD) cell analyzer at the FL1 channel (595 nm). Confocal imaging studies were performed with a Zeiss LSM 510 apochromat confocal laser scanning microscope.

Synthesis. Complexes **1** and **2** were synthesized following a general synthetic procedure in which H_2O_2 (2 drops) was added to an ethanol (25 mL) solution of $Co(CH_3COO)_2{\cdot}4H_2O$ (12.5 mg, 0.05 mmol), followed by addition of a CH_2Cl_2 solution of H_2L (17.3 mg, 0.05 mmol) previously neutralized with Et_3N (0.05 mmol, 6.97 μL). The solution was stirred for 30 min, and Hcur (18.4 mg, 0.05 mmol) or Hmitocur as its dichloride salt (52.3 mg, 0.05 mmol) in ethanol (10 mL) was added. The reaction mixture was stirred for 1 h, filtered, and kept for slow evaporation to isolate a crystalline solid in analytically pure form. The solid was collected by filtration; washed with ice-cold ethanol, cold methanol, and diethyl ether; and finally dried over P_4O_{10} in a vacuum to obtain a brown red solid in ∼80% yield. The characterization data are reported in the following subsections.

DOI: 10.1021/acs.inorgchem.6b00554
Inorg. Chem. XXXX, XXX, XXX−XXX

*Complex [Co^{III}(cur)(L)] (**1**).* Yield = 79%. Anal. Calcd for $C_{55}H_{73}CoN_2O_8$ (M = 948.5): C, 69.58; H, 7.75; N, 2.95. Found: C 69.38; H 7.61; N 3.15. Molar conductivity data in DMF (Λ_M): 14 S m^2 M^{-1}. FT-IR (solid phase): 2945 s, 1585 s, 1510 s, 1460 s, 1400 s, 1370 s,1260 s, 1060 m, 1030 w, 960 w, 880 m, 830 m, 750 w, 730 w, 620 w, 540 m (s, strong; m, medium, w, weak). ESI-MS in MeOH (m/z): 949.4745 $[M + H]^+$. UV−visible in 25% DMF/Tris HCl buffer [λ_{max}/nm (ε/M^{-1} cm^{-1})]: 424 (32900), 297 (22360). Emission in DMSO: 525 nm (Φ = 0.02). ^{1}H NMR (400 MHz, DMSO-d_6): 9.46 (s, 1H), 9.32 (s, 1H), 7.57−6.62 (m, 12H), 6.25 (d, J = 15 Hz, 1H), 6.11 (d, J = 15 Hz, 1H), 5.61 (s, 1H), 3.87 (s, 6H), 3.72 (s, 2H), 3.23 (s, 2H), 3.77 (s, 4H), 2.40 (s, 6H), 1.16−1.12 (m, 36 H) ppm (s, singlet; d, doublet; m, multiplet).

*Complex [Co^{III}(mitocur)(L)]Cl$_2$ (**2**).* Yield = 82%. Anal. Calcd for $C_{97}H_{113}Cl_2CoN_2O_8P_2$ (M = 1626.73): C, 71.62; H, 7.00; N, 1.72. Found: C, 71.86; H, 6.84; N, 1.84. Molar conductivity data in DMF (Λ_M): 152 S m^2 M^{-1}. FT-IR: 2960 s, 1580 w, 1500 s, 1430 s, 1380 m,1250 s, 1020 s, 1020 m, 960 w, 870 w, 800 w, 730 m, 680 m, 500 m. ESI-MS in MeOH (m/z): 777.9482 $[M - 2Cl]^{2+}$. UV−visible in 25% DMF/Tris HCl buffer [λ_{max}/nm (ε/M^{-1} cm^{-1})]: 411 (33330), 275 (34680). Emission in DMSO: 530 nm (Φ = 0.02). ^{1}H NMR (400 MHz, DMSO-d_6): δ 7.78−7.84 (m, 30H), 6.1−7.6 (m, 14H), 5.67 (s, 1H), 3.87 (s, 4H), 3.8 (s, 4H), 3.73 (m, 6H), 2.56 (m, 3H), 2.77 (s, 3H), 2.41 (m, 6H), 2.22 (m, 3H), 1.56−1.54 (m, 3H), 1.17−1.12 (m, 36 H) ppm.

Solubility and Stability. The complexes were soluble in MeOH, DMF, DMSO, MeCN, and aqueous mixtures of these solvents; moderately soluble in $CHCl_3$ and CH_2Cl_2; and insoluble in hydrocarbon solvents. The complexes were stable in both solid and solution phases under dark experimental conditions. The complexes in solution phase were found to release curcumin or mitocurcumin in the presence of a reducing agent, namely, ascorbic acid/glutathione (GSH), or upon photoirradiation with broad-band visible light of 400−700 nm (Luzchem Photoreactor model LZC-1, Ontario, Canada, having Sylvania fluorescent tubes to provide a light dose of 2.4 mW cm^{-2}).

Theoretical Study. The geometry of complex **2** was optimized by density functional theory (DFT) using the B3LYP level of theory with the LanL2DZ basis set for the cobalt center and the 6-31G basis set for all other atoms as implemented in the Gaussian 09 program.[43−45] The initial coordinates were taken from the crystal structure of **1** and were used for the optimization of the structure of complex **2**. The electronic transitions with their transition probabilities were obtained using linear-response time-dependent density functional theory (TDDFT). The coordinates of the energy-minimized structures and selected transitions in the visible region are listed in Tables S1 and S2 (see Supporting Information).

Crystallographic Procedures. The crystal structure of curcumin complex **1** was determined by X-ray diffraction. Single crystals were obtained upon slow evaporation of a methanol/chloroform solution (2:3 v/v) of the complex. A suitable single crystal was mounted on a crystal mounting loop with the help of paratone oil, and the intensity data were collected using graphite-monochromated Mo Kα radiation (0.7107 Å) at 100 K. The structure was solved by direct methods using SHELX-2013 incorporated in WinGX.[46] Empirical absorption corrections were applied with SADABS. All non-hydrogen atoms were refined with anisotropic displacement coefficients.[47] There were three carbon atoms in the structure, namely, C50, C51, and C52, showing positional disorder due to two possible conformations. These carbon atoms were treated in a positional disorder model each with 50% site occupancy. This disorder in the structure had no effect on the chemical properties of the complex. The crystallographic parameters are listed in Table 1. The view of the complex was obtained using ORTEP.[48] CCDC-1434561 contains the crystallographic data for this article.

Cellular Measurements. The cytotoxicity of the complexes was studied using MTT assay in both light and darkness using MCF-7 (breast cancer) and HeLa (cervical cancer) cells following procedures that were reported earlier (see Supporting Information).[4,12,49,50] A cellular incorporation assay was carried out to quantify the cellular uptake of the complexes (10 μM) by flow cytometric analysis in MCF-7 cells following reported procedures.[4,51] The photorelease of mitocurcumin in complex **2** was studied in MCF-7 cells by fluorescence-activated cell sorting (FACS) analysis by quantifying the intracellular curcumin-based fluorescence intensity in different time intervals both in the dark and upon visible-light irradiation (400−700 nm). A 10 μM solution of complex **2** was used for the experiments. DCFDA assay was performed to examine any intracellular ROS formation in MCF-7 cells treated with complex **2** (10 μM) in the light (400−700 nm) and in the dark following standard protocols (see Supporting Information).[51,52] Cellular uptake and localization of complex **2** (10 μM) showing green fluorescence in MCF-7 cells were visualized using a confocal laser scanning microscope (Zeiss, LSM510 apocromat) following standard procedures (see Supporting Information).[4,15,27] Mitochondrial localization was studied using cell-permeable MitoTracker Deep Red FM (catalog no. M22426, 20 nm) to stain the mitochondria.

Table 1. Selected Crystallographic Data for [Co(L)(cur)]·CHCl$_3$ (1·CHCl$_3$)

empirical formula	$C_{56}H_{74}Cl_3CoN_2O_8$
formula weight (g M^{-1})	1068.45
crystal system	triclinic
space group	$P\bar{1}$
a (Å)	9.666(2)
b (Å)	15.854(4)
c (Å)	18.056(3)
α (deg)	84.955(12)
β (deg)	83.52(3)
γ (deg)	88.33(2)
V (Å^3)	2738.1(10)
Z	2
T (K)	100 (2)
ρ_{calc} (g cm^{-3})	1.296
λ (Å) (Mo Kα)	0.71073
μ (cm^{-1})	0.513
data/restraints/parameters	12224/0/659
F(000)	1102
goodness-of-fit	1.042
$R(F_0)$,[a] $I > 2\sigma(I)$ [$R_w(F_0)$][b]	0.0945 [0.2496]
R (all data) [R_w(all data)]	0.1777 [0.3024]
largest diff peak and hole (e Å^{-3})	1.162, −1.509

[a] $R = \sum||F_o| - |F_c||/\sum|F_o|$. [b] $R_w = \sum[w(F_o^2 - F_c^2)^2]/\sum[w(F_o)^2]\}^{1/2}$. $w = [\sigma^2F_o^2 + (AP)^2 + BP]^{-1}$, where $P = (F_o^2 + 2F_c^2)/3$, $A = 0.1933$, and $B = 4.5680$.

RESULTS AND DISCUSSION

Synthesis and General Aspects. Ternary curcumin (Hcur) and mitocurcumin (Hmitocur) cobalt(III) complexes of a dianionic tetradentate phenolate-based ligand (H_2L), namely, [Co(cur)(L)] (**1**) and [Co(mitocur)(L)]Cl$_2$ (**2**), were synthesized in good yields according to a general synthetic procedure in which Co(CH$_3$COO)$_2$ was initially oxidized by H_2O_2 in ethanol, after which H_2L (previously neutralized with Et$_3$N) and Hcur or dicationic Hmitocur in ethanol were added (Figure 1). The complexes were characterized using analytical and spectroscopic data. Selected characterization data are given in Table 2. The ESI-MS spectra of the complexes in methanol showed a single major peak that can be assigned to $[M + H]^+$ for complex **1** and $[M - 2Cl]^{2+}$ for complex **2** (Figures S1 and S2, Supporting Information). The IR spectra of the complexes displayed characteristic stretching bands near 1585 and 1500 cm^{-1} for the C═O and C═C (β-diketonate) moieties, respectively (Figures S3 and S4, Supporting Information).[53]

DOI: 10.1021/acs.inorgchem.6b00554
Inorg. Chem. XXXX, XXX, XXX−XXX

Table 2. Selected Physicochemical Data of Complexes 1 and 2

	1	2
IR[a]/cm^{-1} [$\bar{\nu}$ (C═O)]	1585	1580
electronic:[b] λ_{max}/nm [ε/(M^{-1} cm^{-1})]	424 [32900]	411 [33330]
emission:[c] λ_{em}/nm [Φ]	525 [0.02]	530 [0.02]
Λ_M[d]/(S m^2 M^{-1})	14	152

[a]In KBr phase. [b]Visible electronic spectral band in 25% DMF/Tris HCl buffer. [c]Emission data of the complexes in DMSO with λ_{ex} = 415 nm. Φ is the quantum yield. [d]Λ_M, molar conductance in DMF at 25 °C.

The intense IR band at 1585 cm^{-1} (C═O stretching) indicates bidentate coordination mode of the β-diketone moiety of the cur/mitocur ligand in its enolized form to the central Co(III) center. Complex **1** is nonelectrolytic giving molar conductance value of 14 S m^2 M^{-1} in DMF at 25 °C. Complex **2** is dicationic with a molar conductance value of ∼152 S m^2 M^{-1} in DMF.[54] The complexes are diamagnetic with a low-spin state of the 3d^6 Co(III) ion. ^{1}H NMR spectra of the complexes measured in DMSO-d_6 showed peaks characteristic of the Co(III)-bound *N,N,O,O*-donor L^{2-} and *O,O*-donor cur or mitocur ligands (Figures S5 and S6, Supporting Information). The complexes showed an absorption spectral band near 415 nm in 25% DMF/Tris HCl buffer (Figure 2a). This band is assignable to

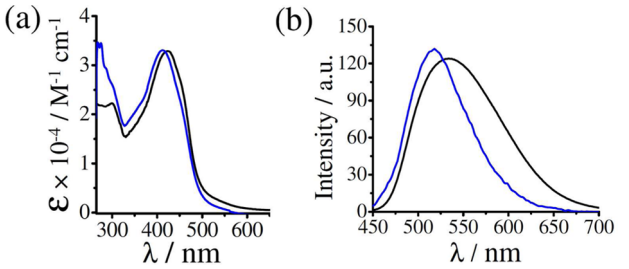

Figure 2. (a) Absorption spectra of complexes **1** (black) and **2** (blue) in 25% DMF/Tris HCl buffer. (b) Fluorescence spectra of complexes **1** (black) and **2** (blue) in DMSO (λ_{ex} = 415 nm).

the curcumin-based $\pi \rightarrow \pi^*$ absorption.[10−13,55] An additional band observed near 280 nm can be assigned to the aromatic $\pi \rightarrow \pi^*$ transition.[4,10−13] Upon excitation at 415 nm, the complexes showed curcumin-based green fluorescence near 525 nm in DMSO with quantum yield (Φ) values in the range of 0.02−0.03 (Figure 2b). The emission property of the curcumin ligands was used to study the cellular uptake and intracellular localization of the complexes by confocal fluorescence microscopy. The redox-active complexes showed an irreversible reduction process assignable to the Co(III)/Co(II) couple near −1.45 V versus SCE in DMF/0.1 M [^{n}Bu$_4$N](ClO$_4$). They also showed curcumin-based quasireversible reduction near −1.74 V. There were no oxidative responses in the cyclic voltammetric scans. The high negative Co^{III}−Co^{II} reduction potential is likely to reduce any facile reduction of the metal by cellular reducing agents such as thiols (GSH) and ascorbic acid. The electrochemical data are of significance with expected reduction of any cellular toxicity of the complexes arising from the release of the metal-bound curcumin ligand in the dark (Figure S7, Supporting Information).[10]

X-ray Crystal Structure. Curcumin complex **1**·CHCl$_3$ was structurally characterized by single-crystal X-ray diffraction. The complex crystallized in the triclinic space group of $P\bar{1}$ with two molecules in the unit cell. The complex has a discrete mononuclear structure with the Co(III) bonded to the *O,O*-donor monoanionic curcumin and the *N,N,O,O*-donor L^{2-}, giving a CoN$_2$O$_4$ coordination arrangement. The complex showed minor positional disorder for three atoms in the tetradentate ancillary ligand. The disordered atoms were refined in two different sets of atoms labeled as A and B and refined with a site occupancy factor of 0.5. A perspective view of the complex having the A set of atoms is shown in Figure 3. (See

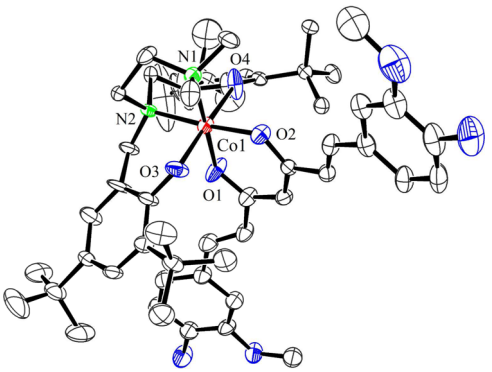

Figure 3. ORTEP view of the cationic complex of **1** with atom labeling scheme for the metal and heteroatoms showing 50% probability thermal ellipsoids. For clarity, hydrogen atoms are not shown.

Figures S8 and S9, Supporting Information, for unit cell packing and the structure with the B set of atoms.) Selected bond distances and angles are given in Table 3. The disorder in the structure had no apparent effect on the chemistry of this complex. At 2.018(4) Å, the Co(1)−N(1) bond is longer than the Co(1)−N(2) bond [1.955(4) Å]. The bonds involving the phenolate oxygen atoms, namely, Co(1)−O(3) and Co(1)−O(4), are 1.897(4) and 1.922(4) Å, respectively. The Co(1)−O(1) and Co(1)−O(2) bonds involving the curcumin ligand are ∼1.88 Å. The M−O(cur) bond distances in the reported curcumin complexes are compared in Table 4.[4,6−8,10] Interestingly, the Co(III)−O(cur) bond distance was found to be the shortest among the structurally characterized metal−curcumin complexes. The observation of a short and strong Co(III)−O(cur) bond is of importance, as the release of the curcumin ligand can be achieved upon reduction of the metal considering that the Co(II)−O(cur) bond is longer and weaker than the Co(III)−O(cur) bond.

Theoretical Studies. Computational studies were performed to rationalize the photophysical properties of the complexes. The energy-optimized structures of the complexes showed that the cobalt(III) center is coordinated to the chelating cur (monoanion of curcumin in **1**) or mitocur (monocation of mitocurcumin in **2**) and the *N,N,O,O*-donor bisphenolate ligand (L), giving a distorted octahedral Co^{III}N$_2$O$_4$ coordination core as observed in the crystal structure of complex **1** (Figure 4a). The bonding parameters are similar to those obtained in the crystal structure. The frontier molecular orbitals (FMOs) of complex **1** showed active participation of the metal center and the tetradentate ligand (L^{2-}) in forming the highest occupied molecular orbitals (HOMOs) and contribution of the curcumin ligand in forming the lowest unoccupied molecular orbitals (LUMOs) (Figure 4b). The HOMO in complex **2** resides primarily on the metal center and the tetradentate ligand (L^{2-}), but the LUMO is

DOI: 10.1021/acs.inorgchem.6b00554
Inorg. Chem. XXXX, XXX, XXX−XXX

Table 3. Selected Bond Distances (Å) and Bond Angles (deg) in [Co(L)(cur)]·$CHCl_3$ (1·$CHCl_3$)

Co(1)–O(1)	1.880(4)	O(1)–Co(1)–O(3)	89.7(2)
Co(1)–O(2)	1.877(4)	O(3)–Co(1)–O(4)	177.8(2)
Co(1)–O(3)	1.920(5)	O(2)–Co(1)–N(2)	92.76(19)
Co(1)–O(4)	1.897(5)	O(1)–Co(1)–N(2)	172.34(18)
Co(1)–N(1)	2.021(5)	O(4)–Co(1)–N(2)	90.9(2)
Co(1)–N(2)	1.956(5)	O(3)–Co(1)–N(2)	91.1(2)
O(2)–Co(1)–O(1)	94.87(19)	O(2)–Co(1)–N(1)	178.4(2)
O(2)–Co(1)–O(4)	88.6(2)	O(1)–Co(1)–N(1)	84.86(19)
O(1)–Co(1)–O(4)	88.5(2)	O(4)–Co(1)–N(1)	89.8(2)
O(2)–Co(1)–O(3)	90.2(3)	O(3)–Co(1)–N(1)	91.4(2)
		N(1)–Co(1)–N(2)	87.5(2)

Table 4. Comparison of the M–O(cur) Bond Distances in Structurally Characterized Curcumin (cur) Complexes

M–O bond	complex[a]	bond distances (Å)	ref
Co–O	[Co(L)(cur)]	1.878(4), 1.880(4)	present work
V–O	[VO(cur)(phen)Cl]	1.973(5), 1.959(4)	4
Zn–O	[Zn(phen)(cur)Cl]	2.016(2), 2.031(2)	6
Ru–O	[(*p*-cymene)Ru(cur)Cl]	2.06(1), 2.07(1)	7
La–O	[La(ph-tpy)(cur)$(NO_3)_2$]	2.400(4), 2.410(4)	12
Gd–O	[Gd(ph-tpy)(cur)$(NO_3)_2$]	2.307(4), 2.315(4)	12

[a]L is the dianion of 6,6′-(((2-(dimethylamino)ethyl)azanediyl)bis(methylene))bis(2,4-di-*tert*-butylphenol) (H_2L), Hcur is curcumin, phen is 1,10-phenanthroline, and the ligand ph-tpy is 4′-(1-pyrenyl)-2,2′:6′,2″-terpyridine.

observed to be located over the triphenylphosphonium (PPh_3^+) cationic moiety.

Stability Study. Curcumin alone is hydrolytically unstable and undergoes rapid degradation in aqueous media with a short half-life of 20 min at pH 7.4, in addition to having poor aqueous solubility.[56] The metal complexes of curcumin are known to be stable under physiological conditions even after 48 h in the dark (Figure S10, Supporting Information). The cobalt(III) complexes showed significant solution stability in the dark as evidenced from the spectral measurements (Figure 5a,b). Additionally, the cellular reducing agents glutathione (GSH) and ascorbic acid, in moderate concentrations up to 10 equiv with respect to the concentration of the complexes, did not show any reduction of the metal to form the cobalt(II) species, possibly because of high negative potential for the Co(III)–Co(II) redox couple. The release of curcumin from the reduced cobalt(II) complexes was previously reported by Hambley and co-workers (Figure 5c).[9] We have observed that an excess concentration of the reducing agents (>10 equiv) showed only partial release of curcumin, as evidenced by an increase in the

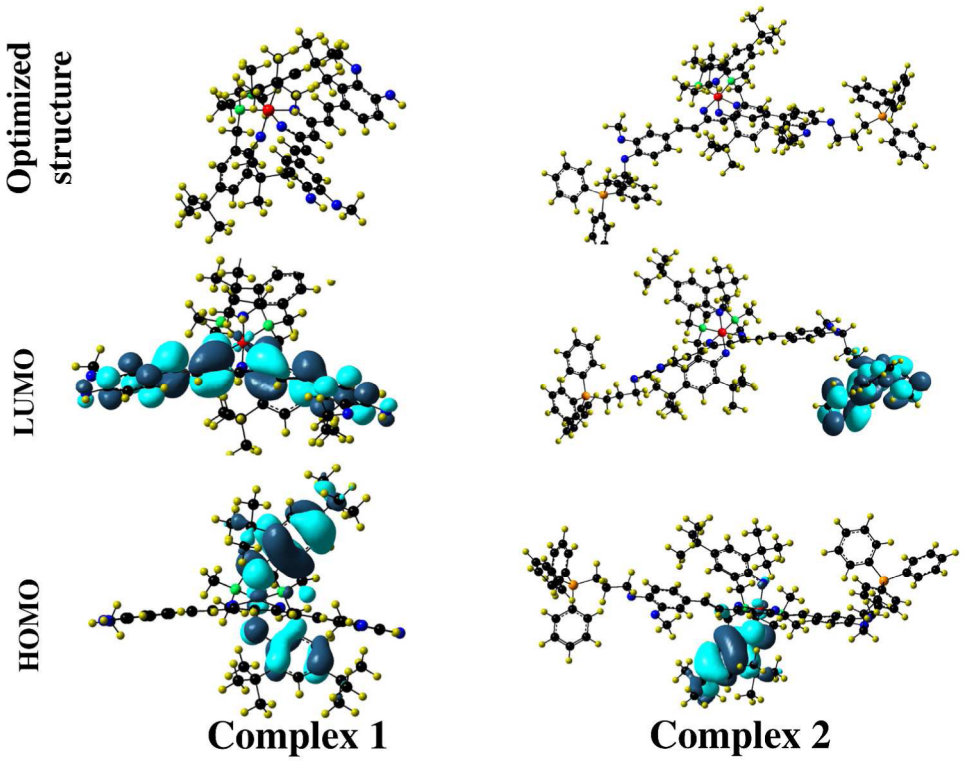

Figure 4. Energy-optimized structures of complexes **1** and **2** along with the FMOs. Color code: C, black; N, green; O, blue; Co, red; H, yellow.

DOI: 10.1021/acs.inorgchem.6b00554
Inorg. Chem. XXXX, XXX, XXX–XXX

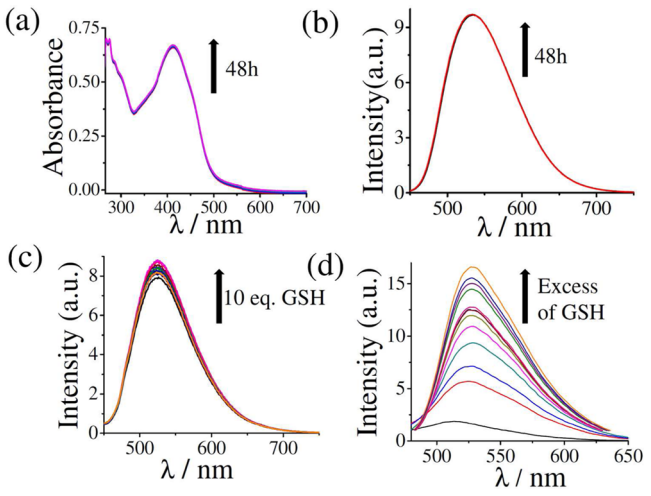

Figure 5. (a) Absorption spectral traces of complex **2** in the dark over a period of 24 h in 25% DMF/Tris HCl buffer (pH 7.2, 37 °C). (b) Emission spectral traces of **2** in the dark over a period of 24 h in 25% DMF/Tris HCl buffer (pH 7.2, 37 °C). (c) Emission spectral traces of **2** upon gradual addition of reduced glutathione up to 10 equiv under similar experimental conditions. (d) Change in the emission spectral traces of **2** upon addition of an excess quantity of reduced glutathione.

fluorescence intensity of the sample over time and the concentration of the reducing agent (Figure 5d). The curcumin dye alone showed higher fluorescence intensity than the ligand in cobalt(III)-bound form. Any release of curcumin thus results in an enhancement of its emission intensity.

Photorelease of Curcumin. Photoinduced ligand substitution or ligand release with concomitant metal reduction is well-known for cobalt(III) and platinum(IV) complexes.[57,58] Photoactivation of the ligand-based $\pi \rightarrow \pi^*$ bands is known to effect electron transfer to the cobalt(III) center.[59] To examine such a possibility for these complexes, 25% DMSO/Tris buffer solutions of the complexes were photoirradiated with visible light at wavelengths of 400−700 nm, and the corresponding changes in the fluorescence spectra were monitored in different time intervals (Figure 6a). Photoirradiation caused a steady increase in the emission intensity of curcumin/mitocurcumin, indicating release of the dye from the complexes. Selective delivery of curcumin inside the cancer cells only upon photoirradiation with visible light is of importance in the chemistry of PDT, as the stability of this dye in metal-bound form in the dark is likely to enhance its in vivo bioavailability.

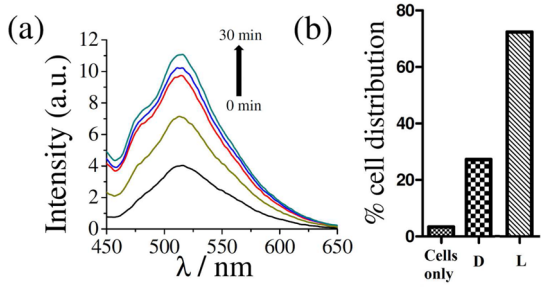

Figure 6. (a) Change in the emission spectral traces of **2** upon irradiation over a period of 30 min in 25% DMSO/Tris HCl buffer (pH 7.2, 37 °C). (b) Enhancement of the intracellular fluorescence intensity of complex-**2**-treated MCF-7 cells upon photoirradiation (400−7000 nm) for 10 min.

The visible-light- (400−700 nm) induced release of mitocurcumin from complex **2** in the cellular environment was studied by FACS analysis to quantify the intracellular curcumin-based fluorescence intensity in MCF-7 cells. A 30-min incubation with complex **2** under darkness showed ∼27% intracellular mitocurcumin-based fluorescence, whereas irradiation with visible light (400−700 nm) for 10 min showed an enhancement in the fluorescence intensity to ∼72%, indicating photorelease of mitocurcumin inside the cells (Figure 6b).

Cellular Uptake and Localization. To examine the cellular permeability and cellular uptake of the complexes and to optimize their incubation time for in vitro cellular studies prior to photoirradiation, a cellular uptake study was carried out using human breast adenocarcinoma (MCF-7) cells at 2- and 4-h time points by fluorescence-activated cell sorting (FACS) analysis in which the intracellular fluorescence of the complex was monitored (Figure 7a). Upon 2 h of incubation, complex **2**

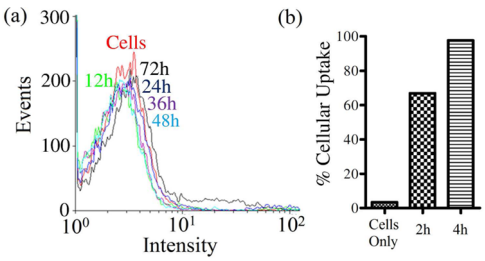

Figure 7. (a) Time-dependent cellular uptake of complex **1** in MCF-7 cancer cells as determined by FACS analysis. (b) Cellular uptake of complex **2** in MCF-7 cells over periods of 2 and 4 h.

showed ∼66.9% cellular uptake, whereas almost complete internalization of this complex was observed within 4 h of incubation (Figure 7b). In contrast, the charge-neutral curcumin complex **1** did not show any significant cellular uptake even after 72 h of incubation (Figure 7a). Interestingly, the curcumin complexes of cobalt(III) in dicationic forms, reported by Hambley and co-workers, are known to show significant cellular uptake.[9] Similarly, the mitocurcumin complex **2** with its dicationic charge showed high cellular uptake. Further studies with additional examples are needed on cobalt(III) curcumin complexes to draw any specific conclusions about the structure−activity relationship in this class of complexes.

Localization of an anticancer drug is of importance to study its pharmacokinetics and to enhance its efficacy.[60−62] Complex **2** being green fluorescent and showing high cellular uptake was chosen for the localization study in the MCF-7 cells by confocal microscopy. The complex with two cationic triphenylphosphonium (TPP) moiety is expected to target the mitochondria of the cells.[39] Confocal images clearly showed the complex predominantly colocalizing with the MitoTracker Deep Red (MTR) suggesting its selective localization in the mitochondria of the cells (Figure 8).

Photoinduced Anticancer Activity. MTT assay was carried out to study the cytotoxicity of the complexes in the dark and upon exposure to visible light using HeLa (human cervical carcinoma) and MCF-7 (human breast adenocarcinoma) cancer cells (Figure 9a; Figures S11 and S12, Supporting Information). Relevant data along with data for other metal−curcumin complexes and photofrin are listed in Table 5.[63] Both of the cobalt(III) complexes were found to be less toxic in the dark. Curcumin complex **1** did not show any toxicity in the

DOI: 10.1021/acs.inorgchem.6b00554
Inorg. Chem. XXXX, XXX, XXX−XXX

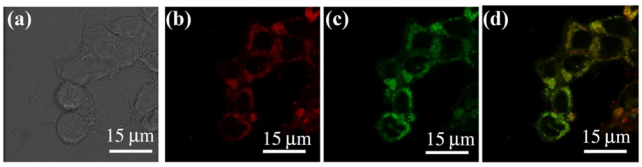

Figure 8. Confocal microscopy images of complex **2** in MCF-7 cells recorded after 4 h of incubation using MitoTracker Deep Red as the staining agent for mitochondria: (a) bright-field image (differential interference contrast), (b) Mitotracker Deep Red (MTR), (c) fluorescence of complex **2**, (d) merged image. Scale bar is 15 μm.

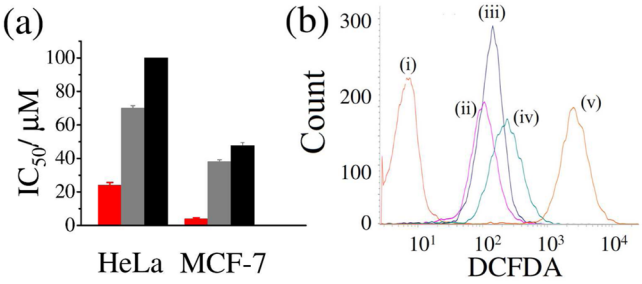

Figure 9. (a) Photocytotoxicity of complex **2** in HeLa and MCF-7 cells upon 4 h of incubation in the dark (black bar), followed by photoirradiation with visible light (400−700 nm, 10 J cm^{-2}) in the absence (red bar) and in the presence of *N*-acetylcysteine (NAC, gray bar). (b) Flow cytometric analysis (FACS) for ROS generation by complex **2** performed using the DCFDA assay in MCF-7 cells treated with complex **2** under different experimental conditions: (i) cells only, (ii) cells + DCFDA, (iii) cells + DCFDA + **2** (in the dark), (iv) cells + DCFDA + complex **2** (in the light), and (v) cells + DCFDA + H_2O_2. A greater shift implies a higher amount of DCF and, thus, greater ROS generation.

Table 5. IC_{50} (μM) Values of the Complexes and Relevant Compounds

complex	IC_{50} (μM)	
	in the light (400−700 nm)	in the dark
1[a]	>100	>100
2[a]	3.9 ± 0.7	50.2 ± 1.4
[Co(cur)(tpa)]ClO_4[b]		39 ± 4
[Co(cur)(tpa-COOH)][c]	6 ± 1	41 ± 4
photofrin[d]	4.3 ± 0.2	>41
cisplatin[e]	−	20.5 ± 0.2

[a]IC_{50} in the light is upon visible-light irradiation (400−700 nm, 10 J cm^{-2}) in MCF-7 cells. Complex **1** showed poor cellular uptake in MCF-7 cells. [b]IC_{50} values in DLD-1 colon cancer cells (from ref 9). [c]IC_{50} values in MCF-7 cells (from ref 18). [d]Values taken from ref 63 for HeLa cells. [e]Value taken from ref 6 for SH-SY5Y cells.

light possibly due to its poor cellular uptake. The mitocurcumin complex **2** showed remarkable PDT activity. It gave an IC_{50} value of >100 μM in HeLa and ∼50 μM in MCF-7 cells on an incubation of 4 h in the dark. Irradiation with a broad-band visible light (400−700 nm) resulted in a significant enhancement of its cytotoxicity, whereas for the untreated light control cells, there was no apparent cell death, thus eliminating the possibility of any cytotoxic effect of the light. Complex **2** gave an IC_{50} value of ∼24.3 μM in HeLa and ∼3.9 μM in MCF-7 cells upon photoactivation. Mitocurcumin alone gave an IC_{50} of ∼3.7 μM in HeLa cells under similar experimental conditions in visible light and ∼13.6 μM in the dark. The dye alone gave an IC_{50} value of ∼1.3 μM in the light and ∼13.7 μM in the dark in MCF-7 cells. The MTT assay data show a significant reduction of the undesired dark toxicity of the mitocurcumin dye on binding to Co(III) while retaining its photocytotoxicity. In addition, a significant reduction in the cytotoxicity was observed in the presence of ROS scavenger *N*-acetylcysteine (NAC), suggesting ROS-mediated anticancer activity.

Curcumin as such or in its metal-bound form is known to generate ROSs upon light activation.[10−14] Being strong oxidizing agents, ROSs oxidize nonfluorescent cell-permeable fluorogenic probe, namely, 2′,7′-dichlorofluorescein diacetate (DCFDA,) to form green fluorescent 2′,7′-dichlorofluorescein (DCF) with an emission maximum at 525 nm that can be monitored by FACS analysis.[64,65] To probe any ROS generation by complex **2**, a DCFDA assay was performed in MCF-7 cells using flow cytometric analysis. Untreated cells did not show any DCF fluorescence. Upon treatment with DCFDA a shift in the intracellular fluorescence corresponding to the basal cellular ROSs. A similar shift in the intracellular fluorescence was also observed when the cells were treated with complex **2** and the dye but kept in the dark. However, cells treated with **2** and exposed to visible light (400−700 nm) for 1 h showed a significant increase in the intracellular emission indicating generation of fluorescent DCF through the ROS-induced oxidation of the nonfluorescent DCFDA (Figure 9b). The cell death event noted with complex **2** in MCF-7 cells is likely to be due to the light-assisted generation of intracellular ROSs.

CONCLUSIONS

Ternary cobalt(III) complexes of curcumin and mitocurcumin having a dianionic tetradentate phenolate-based ancillary ligand were prepared and studied for the photoinduced release of the dye facilitated by concomitant metal reduction. The charge-neutral curcumin complex **1** was structurally characterized by X-ray crystallography. The hydrolytic degradation of curumin and mitocurcumin becomes arrested upon binding to the cobalt(III) ion. This results in an enhanced bioavailability of the dye. A preliminary structure−activity relationship study showed a lower cellular uptake of the neutral curcumin complex **1**, whereas, in contrast, the dicationic mitocurcumin complex **2** displayed significant cellular uptake. This is in agreement with the cellular uptake reported by Hambley and co-workers for cationic cobalt(III) complexes of curcumin. The appendage of two lipophilic cationic triphenylphosphonium (TPP) moieties to the curcumin dye imparts not only higher cellular uptake, but also selective delivery of the complex to the mitochondria of the cells. Complex **2** has shown significant internalization into the mitochondria of the MCF-7 cells with remarkable photoinduced cytotoxicity in visible light with wavelengths of 400−700 nm with a low IC_{50} value (∼3 μM) while being less toxic (>50 μM) when kept in the dark. Studies under extracellular and cellular conditions have revealed photorelease of the dye with metal reduction. The metal in its 3+ oxidation state is, however, not susceptible to reduction even with moderate concentrations of glutathione as a reducing agent. This is due to high negative Co(III)−Co(II) reduction potential observed in the cyclic voltammetric study. Confocal microscopy has revealed both mitochondrial localization of this complex and generation of ROSs which is light-dependent. In summary, this work presents a novel methodology akin to the one reported by Hambley and co-workers to deliver a curcuminiod from a cobalt(III) complex in the cancer cells upon photoactivation in visible light with remarkable PDT

DOI: 10.1021/acs.inorgchem.6b00554
Inorg. Chem. XXXX, XXX, XXX−XXX

activity facilitated by concomitant metal reduction.[18] The results obtained from the SAR study are likely to open up new synthetic designs for PDT prodrugs for intracellular delivery of the therapeutically important curcumin and its derivatives from cobalt(III) complexes.

■ ASSOCIATED CONTENT

Supporting Information

The Supporting Information is available free of charge on the ACS Publications website at DOI: 10.1021/acs.inorgchem.6b00554.

All the details of the experimental procedures, reaction schemes (Schemes S1, S2), mass spectra of the complexes (Figures S1 and S2), IR spectra (Figures S3 and S4), NMR spectra (Figures S5 and S6), cyclic voltammograms (Figure S7), ORTEP views and unit-cell packing diagram (Figures S8 and S9), stability plot of complex **1** (Figure S10), cytotoxicity data of complex **2** (Figures S11 and S12), and calculated energy levels from the theoretical studies (Tables S1 and S2) (PDF)

CIF data for **1**·$CHCl_3$ (CIF)

■ AUTHOR INFORMATION

Corresponding Authors

*E-mail: paturu@mrdg.iisc.ernet.in. Tel.: +91-80-22932688. Fax: +91-80-23600999.

*E-mail: arc@ipc.iisc.ernet.in. Tel.: +91-80-22932533. Fax: +91-80-23600683.

Notes

The authors declare no competing financial interest.

■ ACKNOWLEDGMENTS

We thank the Department of Science and Technology (DST), Government of India, for financial support (SR/S5/MBD-02/2007, EMR/2015/000742). A.R.C. thanks DST for a J. C. Bose national fellowship. We are thankful to the Alexander von Humboldt Foundation, Germany, for the donation of an electroanalytical system. A.G. and S.B. thank IISc, Bangalore, India, for senior research and postdoctoral fellowship, respectively. I.P. acknowledges CSIR for a senior research fellowship. We are thankful to IISc FACS facility and Dr. Santosh Podder for the help extended in confocal microscopy experiments.

■ REFERENCES

(1) Esatbeyoglu, T.; Huebbe, P.; Ernst, I. M. A.; Chin, D.; Wagner, A. E.; Rimbach, G. *Angew. Chem., Int. Ed.* **2012**, *51*, 5308−5332 and references therein.

(2) Grynkiewicz, G.; Ślifirski, P. *Acta Biochim. Pol.* **2012**, *59*, 201−212.

(3) Anand, P.; Thomas, S. G.; Kunnumakkara, A. B.; Sundaram, C.; Harikumar, K. B.; Sung, B.; Tharakan, S. T.; Misra, K.; Priyadarsini, I. K.; Rajasekharan, K. N.; Aggarwal, B. B. *Biochem. Pharmacol.* **2008**, *76*, 1590−1611.

(4) Banerjee, S.; Pant, I.; Khan, I.; Prasad, P.; Hussain, A.; Kondaiah, P.; Chakravarty, A. R. *Dalton Trans.* **2015**, *44*, 4108−4122.

(5) (a) Sharma, R. A.; Steward, W. P.; Gescher, A. J. *Adv. Exp. Med. Biol.* **2007**, *595*, 453−470. (b) Anand, P.; Kunnumakkara, A. B.; Newman, R. A.; Aggarwal, B. B. *Mol. Pharmaceutics* **2007**, *4*, 807−818.

(6) (a) Pucci, D.; Crispini, A.; Mendiguchía, B. S.; Pirillo, S.; Ghedini, M.; Morelli, S.; De Bartolo, L. *Dalton Trans.* **2013**, *42*, 9679−9687. (b) Priyadarsini, K. I. *Molecules* **2014**, *19*, 20091−20112.

(7) Caruso, F.; Rossi, M.; Benson, A.; Opazo, C.; Freedman, D.; Monti, E.; Gariboldi, M. B.; Shaulky, J.; Marchetti, F.; Pettinari, R.; Pettinari, C. *J. Med. Chem.* **2012**, *55*, 1072−1081.

(8) Pettinari, R.; Marchetti, F.; Condello, F.; Pettinari, C.; Lupidi, G.; Scopelliti, R.; Mukhopadhyay, S.; Riedel, T.; Dyson, P. J. *Organometallics* **2014**, *33*, 3709−3715.

(9) (a) Renfrew, A. K.; Bryce, N. S.; Hambley, T. W. *Chem. Sci.* **2013**, *4*, 3731−3739. (b) Bryce, N. S.; Zhang, J. Z.; Whan, R. M.; Yamamoto, M. N.; Hambley, T. W. *Chem. Commun.* **2009**, 2673−2675.

(10) Banerjee, S.; Chakravarty, A. R. *Acc. Chem. Res.* **2015**, *48*, 2075−2083.

(11) Banerjee, S.; Prasad, P.; Hussain, A.; Khan, I.; Kondaiah, P.; Chakravarty, A. R. *Chem. Commun.* **2012**, *48*, 7702−7704.

(12) Hussain, A.; Somyajit, K.; Banik, B.; Banerjee, S.; Nagaraju, G.; Chakravarty, A. R. *Dalton Trans.* **2013**, *42*, 182−195.

(13) Bhattacharyya, A.; Dixit, A.; Mitra, K.; Banerjee, S.; Karande, A. A.; Chakravarty, A. R. *Med. Chem. Commun.* **2015**, *6*, 846−851.

(14) Prasad, P.; Pant, I.; Khan, I.; Kondaiah, P.; Chakravarty, A. R. *Eur. J. Inorg. Chem.* **2014**, *2014*, 2420−2431.

(15) Banerjee, S.; Prasad, P.; Khan, I.; Hussain, A.; Kondaiah, P.; Chakravarty, A. R. *Z. Anorg. Allg. Chem.* **2014**, *640*, 1195−1204.

(16) Banerjee, S.; Dixit, A.; Karande, A. A.; Chakravarty, A. R. *Eur. J. Inorg. Chem.* **2015**, *2015*, 447−457.

(17) Goswami, T. K.; Gadadhar, S.; Gole, B.; Karande, A. A.; Chakravarty, A. R. *Eur. J. Med. Chem.* **2013**, *63*, 800−810.

(18) Renfrew, A. K.; Bryce, N. S.; Hambley, T. *Chem. - Eur. J.* **2015**, *21*, 15224−15234.

(19) Bonnett, R. *Chemical Aspects of Photodynamic Therapy*; Gordon & Breach: London, 2000.

(20) Lovell, J. F.; Liu, T. W. B.; Chen, J.; Zheng, G. *Chem. Rev.* **2010**, *110*, 2839−2857.

(21) Celli, J. P.; Spring, B. Q.; Rizvi, I.; Evans, C. L.; Samkoe, K. S.; Verma, S.; Pogue, B. W.; Hasan, T. *Chem. Rev.* **2010**, *110*, 2795−2838.

(22) Ethirajan, M.; Chen, Y.; Joshi, P.; Pandey, R. K. *Chem. Soc. Rev.* **2011**, *40*, 340−362.

(23) Kamkaew, A.; Lim, S. H.; Lee, H. B.; Kiew, L. V.; Chung, L. Y.; Burgess, K. *Chem. Soc. Rev.* **2013**, *42*, 77−88.

(24) Mari, C.; Pierroz, V.; Ferrari, S.; Gasser, G. *Chem. Sci.* **2015**, *6*, 2660−2686.

(25) Knoll, J. D.; Turro, C. *Coord. Chem. Rev.* **2015**, *282*−*283*, 110−126.

(26) Banerjee, S.; Dixit, A.; Shridharan, R. N.; Karande, A. A.; Chakravarty, A. R. *Chem. Commun.* **2014**, *50*, 5590−5592.

(27) Garai, A.; Basu, U.; Khan, I.; Pant, I.; Hussain, A.; Kondaiah, P.; Chakravarty, A. R. *Polyhedron* **2014**, *73*, 124−132.

(28) Garai, A.; Pant, I.; Kondaiah, P.; Chakravarty, A. R. *Polyhedron* **2015**, *102*, 668−676.

(29) Banerjee, S.; Dixit, A.; Kumar, A.; Mukherjee, S.; Karande, A. A.; Chakravarty, A. R. *Eur. J. Inorg. Chem.* **2015**, *2015*, 3986−3990.

(30) Sarkar, T.; Banerjee, S.; Hussain, A. *RSC Adv.* **2015**, *5*, 16641−16653.

(31) Chakraborty, I.; Carrington, S. J.; Mascharak, P. K. *Acc. Chem. Res.* **2014**, *47*, 2603−2611.

(32) Sarkar, T.; Butcher, R. J.; Banerjee, S.; Mukherjee, S.; Hussain, A. *Inorg. Chim. Acta* **2016**, *439*, 8−17.

(33) Chifotides, H. T.; Dunbar, K. R. *Acc. Chem. Res.* **2005**, *38*, 146−156.

(34) Smith, N. A.; Sadler, P. J. *Philos. Trans. R. Soc., A* **2013**, *371*, 20120519.

(35) Romero-Canelon, I.; Sadler, P. J. *Inorg. Chem.* **2013**, *52*, 12276−12291.

(36) Dhar, S.; Kolishetti, N.; Lippard, S. J.; Farokhzad, O. C. *Proc. Natl. Acad. Sci. U. S. A.* **2011**, *108*, 1850−1855.

(37) Wilson, J. J.; Lippard, S. J. *Chem. Rev.* **2014**, *114*, 4470−4495.

(38) Mitra, K.; Gautam, S.; Kondaiah, P.; Chakravarty, A. R. *Angew. Chem., Int. Ed.* **2015**, *54*, 13989−13993.

(39) Reddy, C. A.; Somepalli, V.; Golakoti, T.; Kanugula, A. K.; Karnewar, S.; Rajendiran, K.; Vasagiri, N.; Prabhakar, S.; Kuppusamy, P.; Kotamraju, S.; Kutala, V. K. *PLoS One* **2014**, *9*, e89351.

DOI: 10.1021/acs.inorgchem.6b00554
Inorg. Chem. XXXX, XXX, XXX−XXX

(40) Clayton, D. A.; Doda, J. N.; Friedberg, E. C. *Proc. Natl. Acad. Sci. U. S. A.* **1974**, *71*, 2777−2781.
(41) Marrache, S.; Pathak, R. K.; Dhar, S. *Proc. Natl. Acad. Sci. U. S. A.* **2014**, *111*, 10444−10449.
(42) Perrin, D. D.; Armarego, W. L. F.; Perrin, D. R. *Purification of Laboratory Chemicals*; Pergamon Press: Oxford, U.K., 1980.
(43) (a) Becke, A. D. *Phys. Rev. A: At., Mol., Opt. Phys.* **1988**, *38*, 3098−3100. (b) Becke, A. D. *J. Chem. Phys.* **1993**, *98*, 5648−5652.
(44) (a) Lee, C.; Yang, W.; Parr, R. G. *Phys. Rev. B: Condens. Matter Mater. Phys.* **1988**, *37*, 785−789. (b) Wadt, W. R.; Hay, P. J. *J. Chem. Phys.* **1985**, *82*, 284−298.
(45) Frisch, M. J.; Trucks, G. W.; Schlegel, H. B.; Scuseria, G. E.; Robb, M. A.; Cheeseman, J. R.; Montgomery, J. A., Jr.; Vreven, T.; Kudin, K. N.; Burant, J. C.; Millam, J. M.; Iyengar, S. S.; Tomasi, J.; Barone, V.; Mennucci, B.; Cossi, M.; Scalmani, G.; Rega, N.; Petersson, G. A.; Nakatsuji, H.; Hada, M.; Ehara, M.; Toyota, K.; Fukuda, R.; Hasegawa, J.; Ishida, M.; Nakajima, T.; Honda, Y.; Kitao, O.; Nakai, H.; Klene, M.; Li, X.; Knox, J. E.; Hratchian, H. P.; Cross, J. B.; Bakken, V.; Adamo, C.; Jaramillo, J.; Gomperts, R.; Stratmann, R. E.; Yazyev, O.; Austin, A. J.; Cammi, R.; Pomelli, C.; Ochterski, J. W.; Ayala, P. Y.; Morokuma, K.; Voth, G. A.; Salvador, P.; Dannenberg, J. J.; Zakrzewski, V. G.; Dapprich, S.; Daniels, A. D.; Strain, M. C.; Farkas, O.; Malick, D. K.; Rabuck, A. D.; Raghavachari, K.; Foresman, J. B.; Ortiz, J. V.; Cui, Q.; Baboul, A. G.; Clifford, S.; Cioslowski, J.; Stefanov, B. B.; Liu, G.; Liashenko, A.; Piskorz, P.; Komaromi, I.; Martin, R. L.; Fox, D. J.; Keith, T.; Al-Laham, M. A.; Peng, C. Y.; Nanayakkara, A.; Challacombe, M.; Gill, P. M. W.; Johnson, B.; Chen, W.; Wong, M. W.; Gonzalez, C.; Pople, J. A. *Gaussian 03*, revision B.4; Gaussian Inc.: Pittsburgh, PA, 2003.
(46) Sheldrick, G. M. *SHELX-2013, Programs for Crystal Structure Solution and Refinement*; University of Göttingen: Göttingen, Germany, 2013.
(47) (a) Walker, N.; Stuart, D. *Acta Crystallogr., Sect. A: Found. Crystallogr.* **1983**, *39*, 158−166. (b) Farrugia, L. J. *J. Appl. Crystallogr.* **1999**, *32*, 837. (c) Farrugia, L. J. *WinGX, version 1.65.04*; Department of Chemistry, University of Glasgow: Glasgow, Scotland, 2003.
(48) Johnson, C. K. *ORTEP-II: A FORTRAN Thermal-Ellipsoid Plot Program for Crystal Structure Illustrations*; Report ORNL-5138; Oak Ridge National Laboratory: Oak Ridge, TN, 1976.
(49) Banerjee, S.; Hussain, A.; Prasad, P.; Khan, I.; Banik, B.; Kondaiah, P.; Chakravarty, A. R. *Eur. J. Inorg. Chem.* **2012**, 3899−3908.
(50) Mosmann, T. *J. Immunol. Methods* **1983**, *65*, 55−63.
(51) Banerjee, S.; Dixit, A.; Karande, A. A.; Chakravarty, A. R. *Dalton Trans.* **2016**, *45*, 783−796.
(52) Sarkar, T.; Banerjee, S.; Hussain, A. *RSC Adv.* **2015**, *5*, 29276−29284.
(53) Nakamoto, K. *Infrared and Raman Spectra of Inorganic and Coordination Compounds*; John Wiley & Sons: New York, 1997.
(54) (a) Geary, W. J. *Coord. Chem. Rev.* **1971**, *7*, 81−122. (b) Ali, I.; Wani, W. A.; Saleem, K. *Synth. React. Inorg., Met.-Org., Nano-Met. Chem.* **2013**, *43*, 1162−1170.
(55) (a) Priyadarsini, I. K. *J. Photochem. Photobiol., C* **2009**, *10*, 81−95. (b) Dahll, T. A.; Bilski, P.; Reszka, K. J.; Chignell, C. F. *Photochem. Photobiol.* **1994**, *59*, 290−294.
(56) Shen, L.; Ji, H.-F. *Trends Mol. Med.* **2012**, *18*, 138−144.
(57) Roundhill, D. M. *Photochemistry and Photophysics of Metal Complexes*; Plenum Press: New York, 1994.
(58) Mackay, F. S.; Woods, J. A.; Heringová, P.; Kašpárková, J.; Pizarro, A. M.; Moggach, S. A.; Parsons, S.; Brabec, V.; Sadler, P. J. *Proc. Natl. Acad. Sci. U. S. A.* **2007**, *104*, 20743−20748.
(59) Funston, A. M.; Cullinane, C.; Ghiggino, K. P.; McFadyen, W. D.; Stylli, S. S.; Tregloan, P. A. *Aust. J. Chem.* **2005**, *58*, 206−212.
(60) Storr, T.; Thompson, K. H.; Orvig, C. *Chem. Soc. Rev.* **2006**, *35*, 534−544.
(61) Noor, F.; Wüstholz, A.; Kinscherf, R.; Metzler-Nolte, N. *Angew. Chem., Int. Ed.* **2005**, *44*, 2429−2432.
(62) Thompson, K. H.; Orvig, C. *Dalton Trans.* **2006**, 761−764.
(63) Delaey, E.; van Laar, F.; De Vos, D.; Kamuhabwa, A.; Jacobs, P.; de Witte, P. *J. Photochem. Photobiol., B* **2000**, *55*, 27−36.
(64) Keston, A. S.; Brandt, R. *Anal. Biochem.* **1965**, *11*, 1−5.
(65) Takanashi, T.; Ogura, Y.; Taguchi, H.; Hashizoe, M.; Honda, Y. *Invest. Ophthalmol. Visual Sci.* **1997**, *38*, 2721−2728.

DOI: 10.1021/acs.inorgchem.6b00554
Inorg. Chem. XXXX, XXX, XXX−XXX